

---

# Papers

---

## The influence of the marine aerosol on atmospheric extinction

OCEANOLOGIA, No. 36 (1)

pp. 3–17, 1994.

PL ISSN 0078–3234

Absorption

Extinction

Marine aerosol

Modified gamma function

JOLANTA KUŚMIERCZYK-MICHULEC  
Institute of Oceanology,  
Polish Academy of Sciences,  
Sopot

Manuscript received May 4, 1994, in final form September 9, 1994.

### Abstract

The simulations presented in this paper were carried out for a range of wavelengths from  $0.3\ \mu\text{m}$  to  $1\ \mu\text{m}$ . Two different size distributions of the marine aerosol are assumed, both represented by the modified gamma function. The parameter values are calculated on the basis of experimental data. Next, modified gamma functions are used to calculate the extinction, scattering and absorption efficiencies. The main result of this paper is that the choice of size distribution of marine aerosols influences the values but not the shapes of functions.

### 1. Introduction

A knowledge of the optical characteristics of atmospheric aerosols (concentration, size distribution, complex refractive index) is a subject of considerable current interest because of its importance to atmospheric radiation processes and their possible effects on our weather and climate.

Many workers have studied the problem of determining the size distribution function  $n(r)$  of a polydispersion. In general, one takes either phase function measurements (Fymat, 1978; Santer *et al.*, 1983) or multispectral extinction measurements on light scattered by the polydispersion (Box and McKellar, 1976, 1979; Klett, 1984) and attempts to obtain the distribution either by direct inversion or by parameter fitting (Shifrin, 1966; McCartney, 1976) in an assumed distribution.

In this paper two aerosol size distributions are assumed, both represented by the modified gamma function. The values of the parameters are found on the basis of experimental data. The modified gamma functions are

then used to calculate the extinction efficiency factor  $Q_{ex}$ , the volume total extinction coefficient  $\beta_{ex}$ , the volume angular scattering coefficient  $\beta(\theta)$ , the backscattering coefficient  $\beta(\pi)$  and the backward scattering coefficient  $b_b$ .

Much of the earlier work (till the 1970s) closely related to the above subject has been reviewed by E. J. McCartney (1976). However, similar work has been done on the aerosol model characterised by the exponential or the power-law size distribution.

This paper presents and discusses the applicable functions, emphasising particularly the dependence of wavelength on attenuation.

This work is regarded as a useful tool in the elaboration and interpretation of satellite data in the visible and near-infrared spectrum, especially as multiplying  $\beta_{ex}$  by the altitude function yields the aerosol optical thickness – a very important parameter in the interpretation of satellite data which has not been sufficiently estimated (Kuśmierczyk-Michulec, 1993).

The experimental data used in this paper were collected by the Institute of Oceanology, Polish Academy of Sciences, in the southern Baltic Sea.

## 2. Aerosol size distribution

The aerosol size distribution can be represented by the modified gamma function (International Association ..., 1984)

$$\frac{dN(r)}{dr} = n(r) = A\left(\frac{r}{r_0}\right)^\alpha \exp\left[-b\left(\frac{r}{r_0}\right)^\gamma\right], \quad (1)$$

where  $N(r)$  is the number of particles with radii smaller than  $r$ ,  $r_0=1 \mu\text{m}$ , and  $A$  is defined such that the total number ( $N_{tot}$ ) of particles is normalised to unity.

In this paper all calculations are carried out simultaneously for two different aerosol size distributions. The first one is described by the expression

$$n_1(r) = A_1\left(\frac{r}{r_0}\right) \exp\left[-b_1\left(\frac{r}{r_0}\right)\right], \quad (2)$$

where  $A_1 = 4247.72 \text{ (cm}^{-3}\text{)}$ ,  $N_{tot} = 10^3 \text{ cm}^{-3}$ ,  $b_1 = 2.06$ ,  $\alpha = 1.0$ ,  $\gamma = 1.0$ .

The second example of aerosol size distribution is defined by the formula

$$n_2(r) = A_2\left(\frac{r}{r_0}\right)^2 \exp\left[-b_2\left(\frac{r}{r_0}\right)\right], \quad (3)$$

where  $A_2 = 15642.83 \text{ (cm}^{-3}\text{)}$ ,  $N_{tot} = 10^3 \text{ cm}^{-3}$ ,  $b_2 = 3.15$ ,  $\alpha = 2.0$ ,  $\gamma = 1.0$ .

The values of the modified gamma function parameters are based on experimental data derived from ‘the measurements by six stage impactors’ (Stramska, 1988), collected by the Polish Institute of Oceanology.

## 3. Mie coefficients

The Mie coefficients yield some important integrated quantities, for example the extinction, scattering and absorption efficiencies. According to

Twomey (1977), the energy removed from an incident wave with energy flux density  $I_0$  is  $\pi r^2 Q_{ex} I_0$ , where  $Q_{ex}$  is the extinction efficiency, the energy reappearing as scattered energy is  $\pi r^2 Q_{sc} I_0$ , where  $Q_{sc}$  is called the scattering efficiency, and the energy absorbed is  $\pi r^2 Q_{ab} I_0$ , where  $Q_{ab}$  is the absorption efficiency.

For simplicity, the ‘anomalous diffraction’ approximation is very often used, which describes the observed light pattern as the interference between straight transmission through the particle and diffraction of the incident light by the particle edge (van de Hulst). This approximation (van de Hulst, 1957) is expressed by

$$Q_{ex} = 2 - 4 \exp[-\rho \tan(\beta)] \left( \frac{\cos(\beta)}{\rho} \right) [\sin(\rho - \beta) + \left( \frac{\cos(\beta)}{\rho} \right) \cos(\rho - 2\beta)] + 4 \left[ \frac{\cos(\beta)}{\rho} \right]^2 \cos(2\beta), \quad (4)$$

where  $\tan(\beta) = \frac{Im(m)}{Re(m)-1}$ ,  $\rho = 2x(Re(m) - 1)$  is the phase-shift parameter describing the phase change of the central light ray crossing the sphere along a diameter,  $x = kr$  is the (dimensionless) size parameter, and  $k = \frac{2\pi}{\lambda}$  is the wave propagation constant. The above approximation is valid when  $m$  is near unity,  $x \gg 1$ , and  $\rho$  is arbitrary but fixed. For  $\beta = 0^\circ$  ( $Im(m) = 0$ ), the above expression reduces to

$$Q_{ex} = Q_{sc} = 2 \left( 1 + \frac{2}{\rho^2} \right) - \frac{4}{\rho} \left( \sin(\rho) + \frac{\cos(\rho)}{\rho} \right). \quad (5)$$

In this paper variations of the extinction efficiency curve  $Q_{ex}(r)$  for several aerosol absorptions are analysed. For marine aerosols, the real part of the complex refractive index in the visible part of spectrum (Fymat *et al.*, 1978) is assumed to be  $Re(m) = 1.33$ .

#### 4. Functions of the modified gamma size distribution

For a case of polydispersion, the basic expression for the total scattering coefficient  $\beta_{sc}$  is the integrand over the selected size distribution

$$\beta_{sc} = \pi \int_{r_1}^{r_2} r^2 Q_{sc} n(r) dr. \quad (6)$$

An analogous expression for the extinction  $\beta_{ex}$  is obtained by employing  $Q_{ex}$  instead of  $Q_{sc}$ :

$$\beta_{ex} = \pi \int_{r_1}^{r_2} r^2 Q_{ex} n(r) dr. \quad (7)$$

The volume scattering function  $\beta(\theta)$  for a polydispersion is defined as

$$\beta(\theta) = P(\theta) \frac{\beta_{sc}}{4\pi}, \quad (8)$$

where  $P(\theta)$  is the phase function for a suspension of particles. The aerosol phase function  $P(\theta)$  can be defined by the two-term Henyey–Greenstein (TTHG) function (Guzzi *et al.*, 1987):

$$P(\theta) = \frac{(1 - g_1^2)a}{(1 + g_1^2 - 2g_1 \cos(\theta))^{1.5}} + \frac{(1 - g_2^2)(1 - a)}{(1 + g_2^2 + 2g_2 \cos(\theta))^{1.5}}, \quad (9)$$

where  $a$ ,  $g_1$ ,  $g_2$  define the type of aerosol used in the evaluation of the scattering process and, according to Gordon (Guzzi *et al.*, 1987), for the marine aerosol  $a = 0.985$ ,  $g_1 = 0.713$ , and  $g_2 = 0.759$ .

In this paper, the volume scattering function  $\beta(\theta)$  was used in order to calculate the backscattering coefficient  $\beta(\pi)$  and the backward scattering coefficient  $b_b$  for two different aerosol size distributions.

The backward scattering coefficient is expressed by

$$b_b = 2\pi \int_{(\frac{\pi}{2})}^{\pi} \beta(\theta) \sin(\theta) d\theta. \quad (10)$$

## 5. Results

Many workers have studied the wavelength dependence of attenuation by haze; much of the earlier work has been reviewed by McCartney (1976). Generally, studies of marine aerosol scattering have been based on the exponential or the power-law size distribution. The results presented in this paper are based on the modified gamma function.

Fig. 1 presents the aerosol size distribution for two modified gamma functions used in further calculations.

Fig. 2 shows  $Q_{sc}$  as a function of the wavelength for various particle radii from  $r = 0.01 \mu\text{m}$  to  $r = 1.0 \mu\text{m}$ . It is clear that the most important influence on scattering in the visible spectrum is exerted by a suspension of very small particles (0.3 to 0.5  $\mu\text{m}$ ). The total scattering cross-section of tinier particles are too small to have any influence; larger particles also have little influence because their concentration is too low.

Fig. 3a to 3c show variations in the extinction efficiency curve  $Q_{ex}(r)$  for several aerosol absorptions in the visible spectrum. The real part of the complex refractive index is assumed to be  $Re(m) = 1.33$ . The imaginary component of this quantity increases from  $Im(m) = 0.088$  ( $\beta = 15^\circ$ ), through  $Im(m) = 0.19$  ( $\beta = 30^\circ$ ), to  $Im(m) = 0.33$  ( $\beta = 45^\circ$ ). The strong damping effect with the increase in absorption for particle radii  $r \geq 5 \mu\text{m}$  is evident. As a general conclusion, it can be stated that for particle radii  $r > 5 \mu\text{m}$  (Figs. 3a, 3d), the value of the imaginary part of the complex

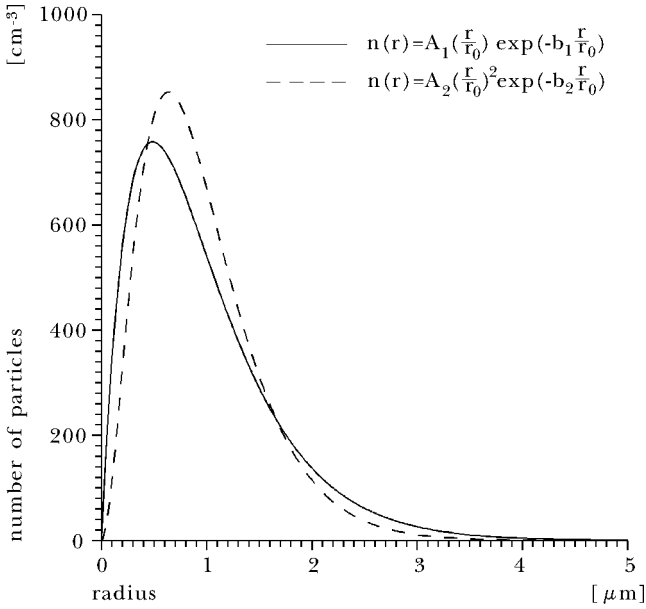


Fig. 1. The aerosol size distribution for two modified gamma functions

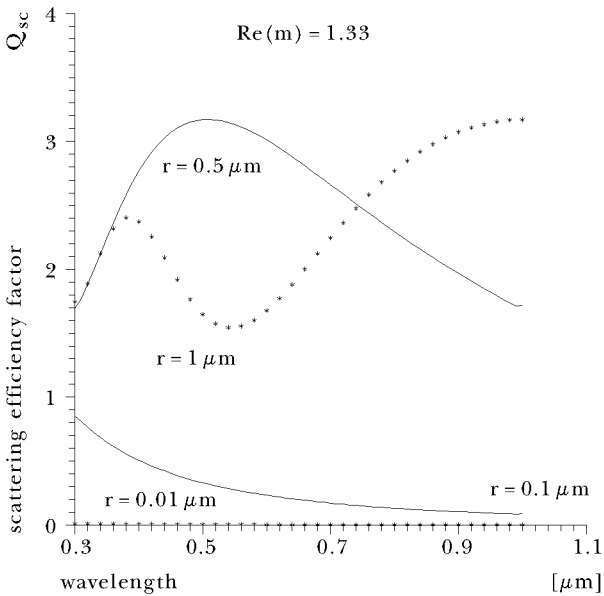
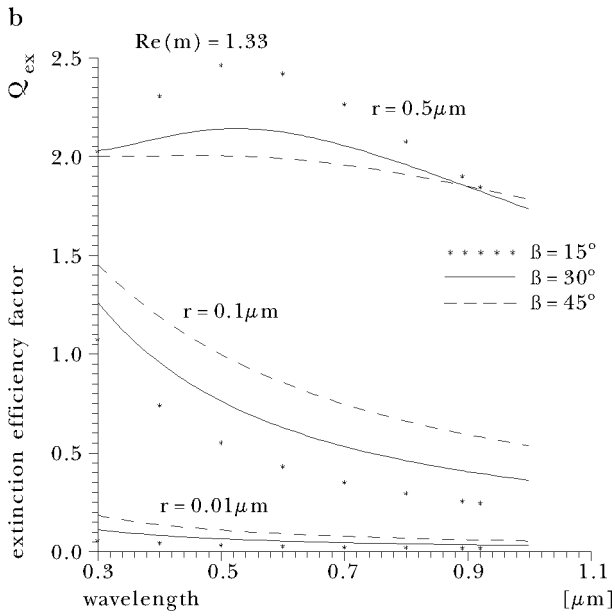
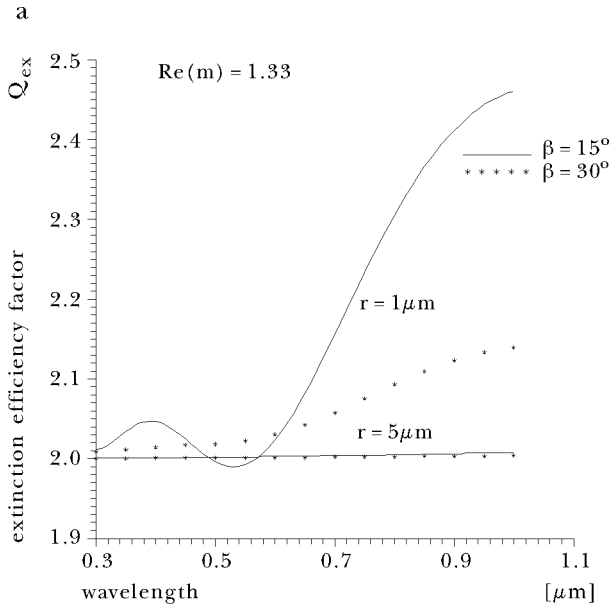


Fig. 2. Spectra of the scattering efficiency factor  $Q_{sc}$  for various particle radii from  $r = 0.1 \mu\text{m}$  to  $r = 1 \mu\text{m}$ ; the real part of the complex refractive index is assumed to be  $Re(m) = 1.33$ , the imaginary part  $Im(m) = 0$



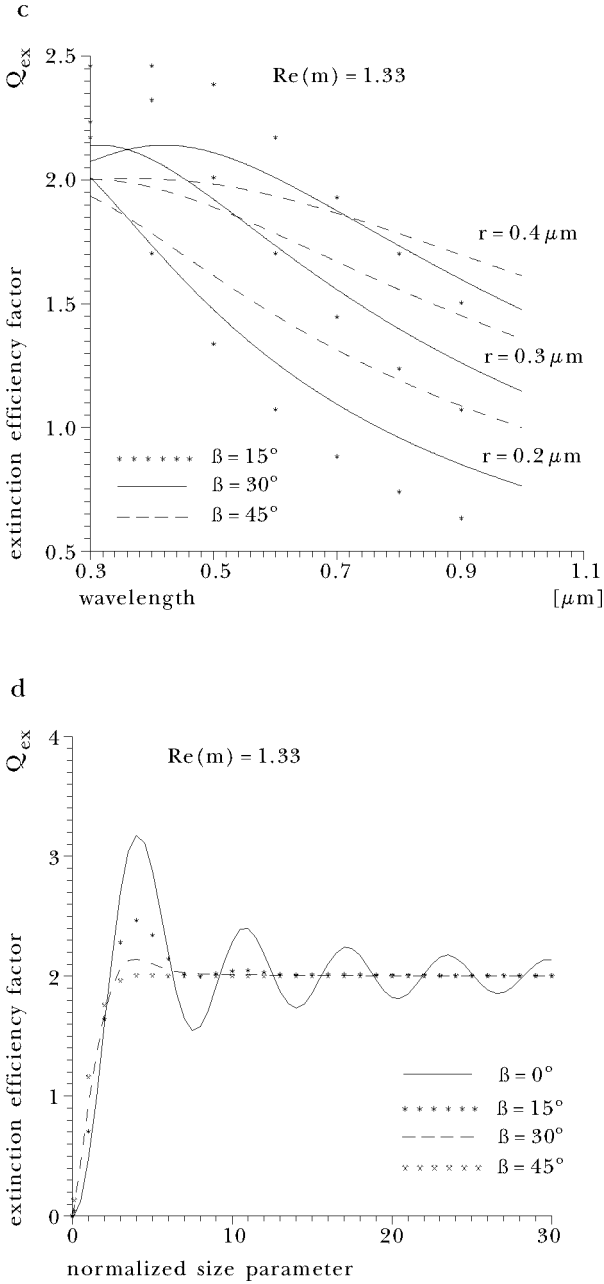


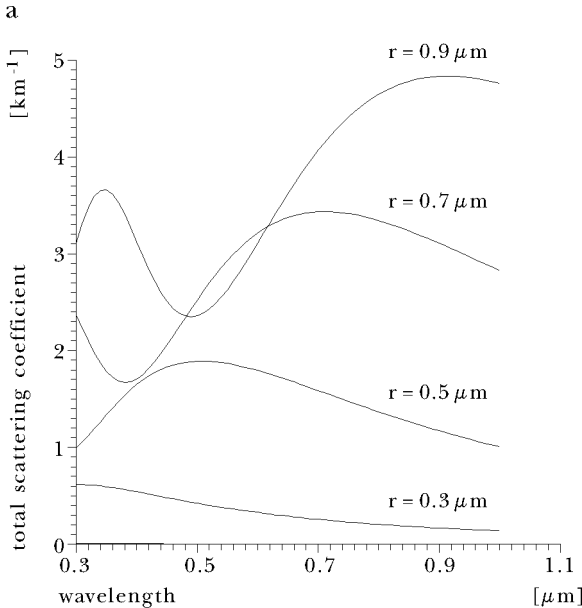
Fig. 3. Spectra of the extinction efficiency factor  $Q_{ex}$  for several aerosol absorption and various particle radii: two values of absorption  $\beta$ :  $15^\circ$ ,  $30^\circ$ , and two values of particle radius  $r = 1, 5 \mu m$  (a), three values of  $\beta$ :  $15^\circ$ ,  $30^\circ$ ,  $45^\circ$ , and three values of  $r$ :  $0.01, 0.1, 0.5 \mu m$  (b), three values of  $\beta$ :  $15^\circ$ ,  $30^\circ$ ,  $45^\circ$  and three values of  $r$ :  $0.2, 0.3, 0.4 \mu m$  (c), extinction efficiency factor for the normalised size parameter (d)

refractive index has no influence on the shape of function  $Q_{ex}$ . Different values of  $Im(m)$  give the same result  $Q_{ex} = 2$ . Fig. 3d presents the above effect for the normalised size parameter. As this increases,  $Q_{ex}$  rises to a maximum of nearly 3.2 (for  $Im(m) = 0$ ) and then slowly converges to the value 2 in the manner of a damped oscillation.

For absorption  $\beta = 30^\circ$  and particle radius  $r = 1 \mu\text{m}$ ,  $Q_{ex}$  can be described by the exponential function  $Q_{ex} = 1.9 \exp(0.1\lambda)$ ; for  $r = 5 \mu\text{m}$  each value of absorption yields  $Q_{ex} = 2$  (Fig. 3a). For particles smaller than  $r = 0.3 \mu\text{m}$  (Fig. 3b, 3c), the values of  $Q_{ex}$  can be described by the following decreasing exponential function (Fig. 3b):

$$\begin{aligned} \text{if } r = 0.01 \mu\text{m} & \quad \text{and } \beta = 15^\circ, & Q_{ex} = 0.08 \exp(-1.77\lambda), \\ \text{if } r = 0.01 \mu\text{m} & \quad \text{and } \beta = 30^\circ, & Q_{ex} = 0.16 \exp(-1.68\lambda), \\ \text{if } r = 0.01 \mu\text{m} & \quad \text{and } \beta = 45^\circ, & Q_{ex} = 0.26 \exp(-1.62\lambda), \\ \text{if } r = 0.1 \mu\text{m} & \quad \text{and } \beta = 15^\circ, & Q_{ex} = 1.7 \exp(-2.16\lambda), \\ \text{if } r = 0.1 \mu\text{m} & \quad \text{and } \beta = 30^\circ, & Q_{ex} = 1.86 \exp(-1.72\lambda), \\ \text{if } r = 0.1 \mu\text{m} & \quad \text{and } \beta = 45^\circ, & Q_{ex} = 2.05 \exp(-1.39\lambda). \end{aligned}$$

For particle radii  $r > 0.3 \mu\text{m}$ , the ‘inversion effect’ is observed – the higher the absorption, the lower the extinction efficiency. The limiting value of particle radius for the ‘inversion effect’ can be assumed to be  $r = 0.3 \mu\text{m}$  (Figs. 3b, 3c).





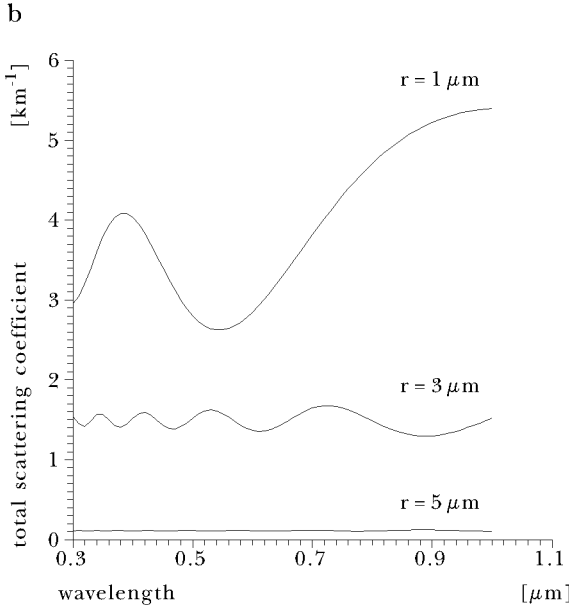


Fig. 4. Spectra of the total scattering coefficient  $\beta_{sc}$  for several aerosol absorption and various particle radii:  $\beta_{sc}$  calculated for  $r : 0.3, 0.5, 0.7, 0.9 \mu\text{m}$  (a),  $\beta_{sc}$  presented for  $r : 1.0, 3.0, 5.0 \mu\text{m}$  (b)

Fig. 4a to 4b show  $\beta_{sc}$  as a function of the wavelength for various particle radii. It is clear that only for a suspension of very small or very large particles can the dependence be a simple function for a broad range of wavelengths. Moreover, in the visible and near-infrared spectrum, *i.e.* from  $0.3 \mu\text{m}$  to  $1 \mu\text{m}$ , particles with  $0.3 \mu\text{m} < r \leq 1 \mu\text{m}$  have the most important influence on scattering.

Next, the respective dependences on wavelengths for the backscattering coefficient  $\beta_{(\pi)}$  and backward scattering coefficient  $b_b$  are presented. It should be stressed that for two different aerosol size distributions, the curve shapes in both cases remains unchanged, only the values are shifted (Figs. 5, 6). It is enough to choose one of these two aerosol size distributions and multiply the result of  $\beta_{(\pi)}$  or  $b_b$  respectively, by the constant.

Fig. 7a to 7c show the total extinction coefficient  $\beta_{ex}$  as a function of wavelength (from  $0.3 \mu\text{m}$  to  $1 \mu\text{m}$ ) for various particle radii and for several aerosol absorptions.

The best fits are

$$\text{for } r = 1 \mu\text{m} \text{ and } \beta = 15^\circ \quad \beta_{ex} = 0.85 + 21.9\lambda - 65.2\lambda^2 + 79.9\lambda^3 - 33.3\lambda^4$$

(Fig. 7a),

$$\begin{aligned}
&\text{for } r = 1 \mu\text{m and } \beta = 30^\circ & \beta_{ex} &= 3.26 + 0.36\lambda & (\text{Fig. 7a}), \\
&\text{for } r = 1 \mu\text{m and } \beta = 45^\circ & \beta_{ex} &= 3.39 + 0.01\lambda & (\text{Fig. 7a}), \\
&\text{for } r = 0.3 \mu\text{m and } \beta = 15^\circ & \beta_{ex} &= 0.8\exp(-1.5\lambda) & (\text{Fig. 7b}), \\
&\text{for } r = 0.5 \mu\text{m and } \beta = 15^\circ & \beta_{ex} &= -0.5 + 9\lambda - 12.7\lambda^2 + 5.3\lambda^3 & (\text{Fig. 7b}), \\
&\text{for } r = 0.7 \mu\text{m and } \beta = 15^\circ & \beta_{ex} &= 2.4 - 3.4\lambda + 9.8\lambda^2 - 6.6\lambda^3 & (\text{Fig. 7b}), \\
&\text{for } r = 0.9 \mu\text{m and } \beta = 15^\circ & \beta_{ex} &= 5.6 - 14.4\lambda + 24.5\lambda^2 - 12\lambda^3 & (\text{Fig. 7b}), \\
&\text{for } r = 0.3 \mu\text{m and } \beta = 30^\circ & \beta_{ex} &= 0.5 - 0.3\lambda & (\text{Fig. 7c}), \\
&\text{for } r = 0.5 \mu\text{m and } \beta = 30^\circ & \beta_{ex} &= 1.4 - 0.3\lambda & (\text{Fig. 7c}), \\
&\text{for } r = 0.7 \mu\text{m and } \beta = 30^\circ & \beta_{ex} &= 2.2 + 0.1\lambda & (\text{Fig. 7c}), \\
&\text{for } r = 0.9 \mu\text{m and } \beta = 30^\circ & \beta_{ex} &= 2.9 + 0.4\lambda & (\text{Fig. 7c}).
\end{aligned}$$

As a general conclusion it can be stated that for absorption  $\beta = 45^\circ$ , the integrand  $\pi r^2 Q_{ex} n(r)$  approximates to a constant value. However, for  $\beta = 30^\circ$ , the above integrand can be substituted (with negligible error) for a linear function.

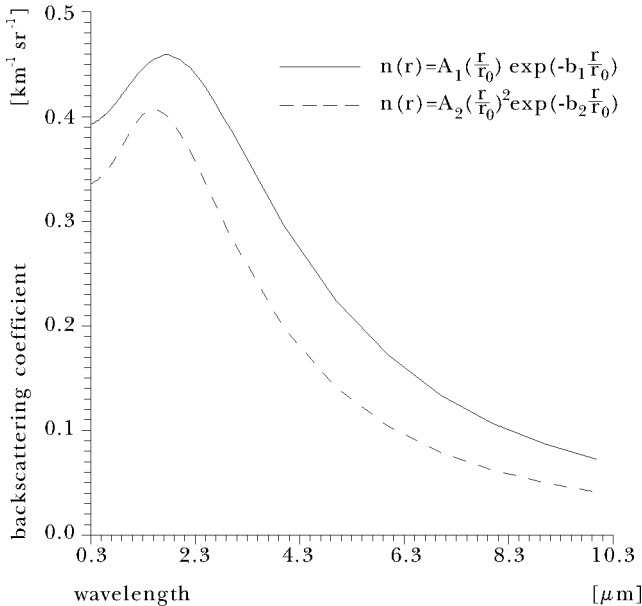


Fig. 5. The backscattering coefficient  $\beta(\pi)$  as a function of wavelength  $\lambda$  for two different aerosol size distributions

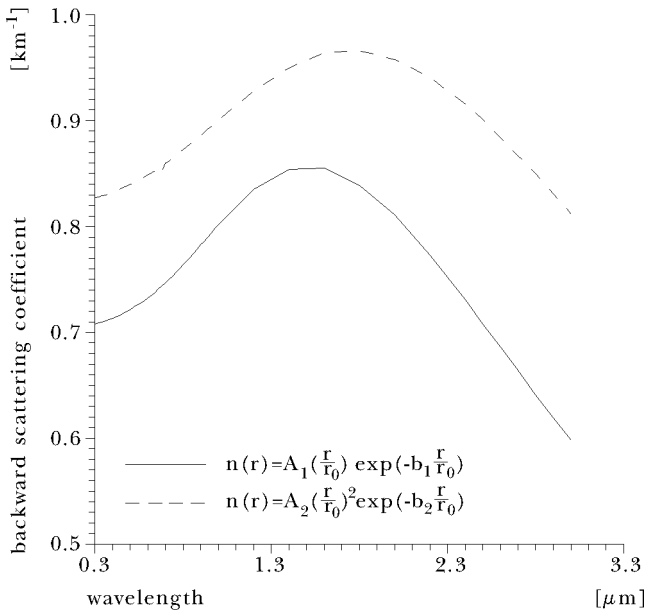
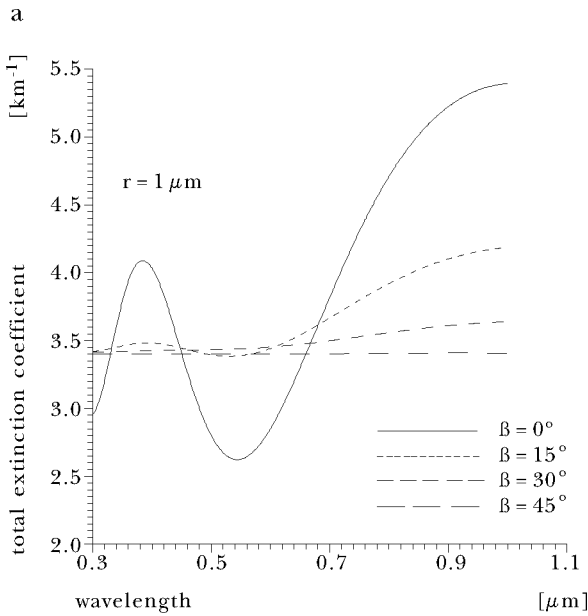


Fig. 6. The backward scattering coefficient  $b_b$  as a function of wavelength  $\lambda$  for two different aerosol size distributions



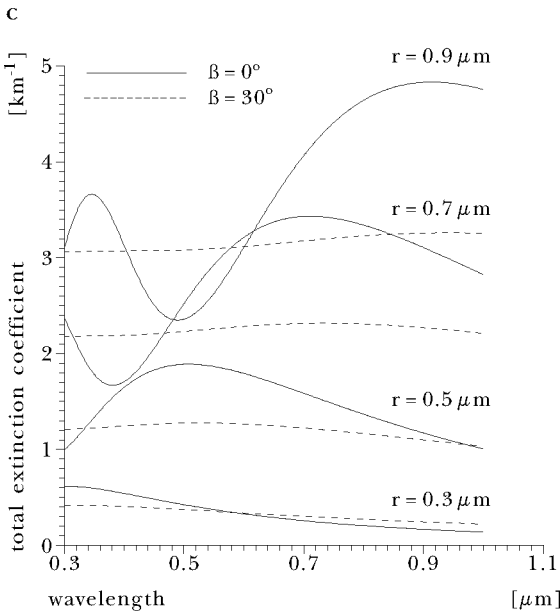
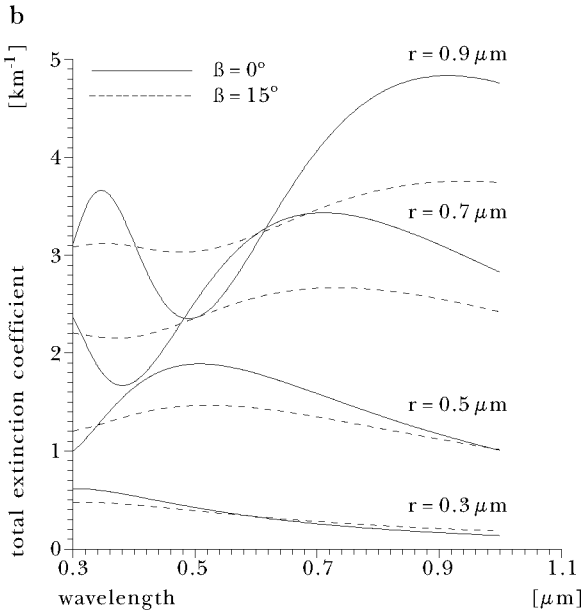


Fig. 7. Total extinction coefficient as a function of wavelength, from  $0.3\mu\text{m}$  to  $1\mu\text{m}$ , for various particle radii and for several aerosol absorptions:  $\beta_{ex}$  for  $r = 1\mu\text{m}$  and for various absorptions (a), extinction for two values of  $\beta : 0^\circ, 15^\circ$  (b),  $\beta_{ex}$  for two values of  $\beta : 0^\circ, 30^\circ$  (c)

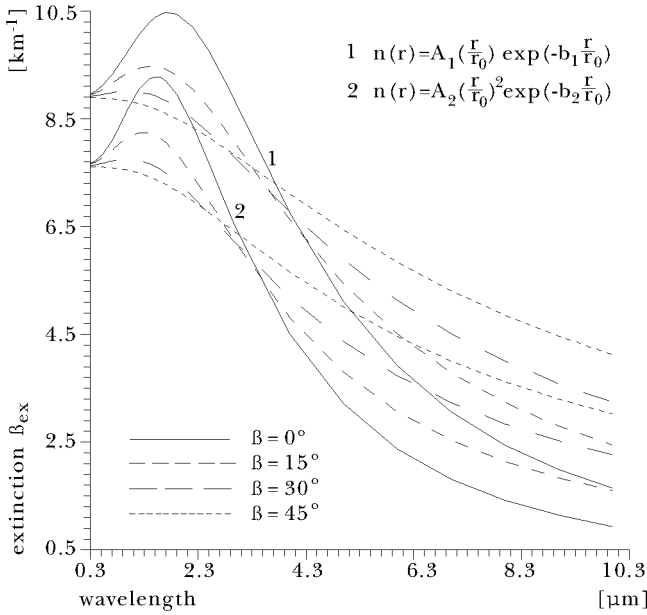


Fig. 8. The extinction  $\beta_{ex}$  as a function of wavelength  $\lambda$  for two different aerosol size distributions and for several aerosol absorptions

Finally, Fig. 8 presents  $\beta_{ex}$  for two aerosol size distributions and for several aerosol absorptions over a broad range of wavelengths (from  $0.3 \mu\text{m}$  to  $10 \mu\text{m}$ ).  $\beta_{ex}$  can be substituted for the following polynomials:

if  $n(r) = A_1 \left(\frac{r}{r_0}\right) \exp\left[-b_1 \left(\frac{r}{r_0}\right)\right]$  and

$$\beta = 0^\circ, \quad \beta_{ex} = 7.6 + 3.6\lambda - 1.6\lambda^2 + 0.2\lambda^3 - 0.01\lambda^4,$$

$$\beta = 15^\circ, \quad \beta_{ex} = 8.3 + 1.9\lambda - 0.98\lambda^2 + 0.1\lambda^3 - 0.005\lambda^4,$$

$$\beta = 30^\circ, \quad \beta_{ex} = 8.7 + 0.8\lambda - 0.6\lambda^2 + 0.07\lambda^3 - 0.003\lambda^4,$$

$$\beta = 45^\circ, \quad \beta_{ex} = 8.9 - 0.05\lambda - 0.1\lambda^2 + 0.01\lambda^3,$$

if  $n(r) = A_2 \left(\frac{r}{r_0}\right)^2 \exp\left[-b_2 \left(\frac{r}{r_0}\right)\right]$  and

$$\beta = 0^\circ, \quad \beta_{ex} = 6 + 4.8\lambda - 2.5\lambda^2 + 0.4\lambda^3 - 0.03\lambda^4 + 0.001\lambda^5,$$

$$\beta = 15^\circ, \quad \beta_{ex} = 6.8 + 2.75\lambda - 1.7\lambda^2 + 0.3\lambda^3 - 0.025\lambda^4 + 0.0007\lambda^5,$$

$$\beta = 30^\circ, \quad \beta_{ex} = 7.3 + 1.3\lambda - 0.9\lambda^2 + 0.2\lambda^3 - 0.01\lambda^4 + 0.0004\lambda^5,$$

$$\beta = 45^\circ, \quad \beta_{ex} = 7.7 - 0.1\lambda - 0.1\lambda^2 + 0.01\lambda^3.$$

Obviously, the values of  $\beta_{ex}$  for two aerosol size distributions have shifted (as in Fig. 5, 6) Moreover, this feature is characteristic of different values of absorption. Then, the main result of this work is that the choice of size distribution has an influence only on the value not on the shape of a function.

## 6. Conclusions

The simulations presented in this paper were carried out for a wide range of wavelengths from  $0.3\ \mu\text{m}$  to  $1\ \mu\text{m}$ . The main conclusion of this paper is that the choice of size distribution of a marine aerosol influences the values, not the shape of the function. Moreover, the ‘error’ associated with the determination of  $\beta(\pi)$ ,  $b_b$  or  $\beta_{ex}$  by one of two aerosol size distributions is relatively small.

On the other hand, the proper choice of aerosol size distribution and refractive index is very important, because it has a direct influence on the extinction. The latter quantity multiplied by the altitude function becomes the aerosol optical thickness – a very important parameter in the interpretation of satellite data.

This work is considered a useful tool in elaborating and interpreting satellite data in the visible and near-infrared spectrum, especially as two of five AVHRR channels have similar spectral bands, *i.e.* the  $0.58 - 0.68\ \mu\text{m}$  and  $0.725 - 1.10\ \mu\text{m}$  bands. Moreover, nearly all (five of six) of the CZCS channels are included in this range.

## 7. Acknowledgments

I would like to thank Prof. A. Zieliński for giving me the idea of such a paper and for discussions on individual questions. I also thank Mr. C. Michulec for his personal support.

## References

- Box M. A., McKellar B. H. J., 1976, *Determination of moments of the size distribution function in scattering by polydispersions*, Appl. Opt., 15 (11), 2610.
- Box M. A., McKellar B. H. J., 1979, *Relationship between two analytic inversion formulae for multispectral extinction data*, Appl. Opt., 18 (21), 3599–3601.
- Fymat A. L., 1978, *Analytical inversions in remote sensing of particle size distributions. 2: Angular and spectral scattering in diffraction approximations*, Appl. Opt., 17 (11), 1677–1678.
- Fymat A. L., Mease K. D., 1978, *Complex refractive index of atmospheric aerosols: a size distribution independent retrieval approach using multispectral transmission ratios* [in:] *Remote sensing of the atmosphere: inversion methods and applications*, A. L. Fymat and V. E. Zuyev (eds.), Elsevier, Amsterdam–Oxford–New York, 233–256.
- Guzzi R., Rizzi R., Zibordi G., 1978, *Atmospheric correction of data measured by a flying platform over the sea: elements of a model and its experimental validation*, Appl. Opt., 26 (15), 3043–3051.
- van de Hulst H. C., 1957, *Light scattering by small particles*, Wiley, New York, 176–179.

- 
- International Association for Meteorology and Atmospheric Physics, Radiation Commission, 1984, *A preliminary cloudless standard atmosphere for radiation computation*, Boulder, Colorado, USA, 9–10.
- Klett J. D., 1984, *Anomalous diffraction model for inversion of multispectral extinction data including absorption effects*, Appl. Opt., 23 (24), 4499–4508.
- Kuśmierczyk-Michulec J., 1993, *The aerosol optical thickness of the atmosphere over the Norwegian Sea obtained from different experimental data*, Oceanologia, 34, 27–37.
- McCartney E. J., 1976, *Optics of the atmosphere; scattering by molecules and particles*, J. Wiley and Sons, New York, 200–314.
- Santer R., Herman M., 1983, *Particle size distributions from forward scattered light using the Chahine inversion scheme*, Appl. Opt., 22 (15), 2294–2301.
- Shifrin K. S., Perelman A. Y., 1966, *Determination of particle spectrum of atmosphere aerosol by light scattering*, Tellus, 18, 566.
- Stramska M., 1988, *On the method of measurement of concentration and distribution of marine aerosol particle sizes using an impactor*, Stud. i Mater. Oceanol., 53, 247–268, (in Polish).
- Twomey S., 1977, *Atmospheric aerosols*, Elsevier, Amsterdam–Oxford–New York, 208–209.